

Electronic Supplementary Information

**A Novel Ammonium Pentaborate – Poly(ethylene-glycol)
Templated Polymer-Inclusion Compound**

Anna R. Ploszajski, Matthew Billing, Neal T. Skipper and Jeremy K. Cockcroft

Table of Contents

Page No.

Additional Experimental Details

Single crystal X-ray diffraction measurements and analysis.

1

Additional Discussion

Mechanism of formation

2

List of Tables

SXD data on $\text{NH}_4\text{B}_5\text{O}_6(\text{OH})_4 \cdot (\text{C}_2\text{H}_4\text{O})_x$ at 150 K.

Table S1. Crystal data and structure refinement.	4
Table S2. Fractional atomic coordinates and $U(\text{eq})$ for all atoms.	5
Table S3. Anisotropic displacement parameters.	6
Table S4. Table of selected bond lengths.	7
Table S5. Table of selected bond angles.	7
Table S6. Solvent mask information.	8

List of Figures

Fig. S1. Motif of the crystal showing the labelling scheme of the atoms.	8
Fig. S2. View along a in the crystal showing the PEO containing channels.	9
Fig. S3. Two views of the crystal used in the experiment.	10

Single crystal X-ray diffraction measurements and analysis

A single crystal of the prepared cocrystal was held in a Hampton Research nylon loop (20 μm thickness, 0.3 mm diameter, as shown in Fig. S3). The sample was cooled to 150 K and measurements were made using a twin-source SuperNova diffractometer with a micro-focus Cu K α X-ray beam (50 kV, 0.8 mA), an Atlas (135 mm CCD) detector, and the sample temperature was controlled with an Oxford Instruments Cryojet5. A half sphere of data was collected at 30 s per 1° frame for low angle data and at 120 s per 1° frame for high angle data with a total data collection time of around 17 hr. The data were processed with the CrysAlisPro software package (version 1.171.38.43) from Rigaku Oxford Diffraction. The crystal structure was solved using charge flipping¹ and refined by least-squares within the Olex2 program suite² using ShelXL from the 2014 refinement program suite.³ For the NH₄⁺ cations, H atom positions and isotropic displacement were refined with equal distance and displacement restraints; for the OH groups, H atoms were fixed using idealized tetrahedral geometry. Due to extensive disorder within the channels formed by the pentaborate

¹ L. Palatinus, S. J. Prathapa and S. van Smaalen, *J. Appl. Crystallogr.* 2012, **45**, 575-580.

² O. V. Dolomanov, L. J. Bourhis, R. J. Gildea, J. A. K. Howard and H. Puschmann, *J. Appl. Crystallogr.* 2009, **42**, 339-341.

³ G. M. Sheldrick, *Acta Crystallogr.* 2015, **C71**, 3-8.

framework anions, electron density due to the PEG molecule chains within the channels was accounted for using the “squeeze” option within Olex2 with the solvent and shrink radius set to 1.2 Å.⁴

Mechanism of formation of $\text{NH}_4\text{B}_5\text{O}_6(\text{OH})_4 \cdot x(\text{C}_2\text{H}_4\text{O})$.

The transformation of a mixture of AB and PEG powders into the structure reported here is complex and involves a number of steps. The first of these processes begins with the melting of the AB-PEG mixture, resulting in instantaneous hydrogen release. The decomposition of AB in the presence of ether compounds has been well studied in the literature,⁵ and in the liquid polyether environment, AB rapidly decomposes to aminoborane (NH_2BH_2 , AoB) and H_2 (Eq. 1). This AoB species is highly reactive and rapidly oligomerises to form polyaminoborane (PAB) compounds such as cyclotriborazane ($\text{B}_3\text{N}_3\text{H}_{12}$, CTB) (Eq. 2). Competing hydrogen transfer reactions (Eq. 3) and dehydrogenation processes (Eq. 4) then produce reactive borazine ($\text{B}_3\text{N}_3\text{H}_6$, BZ) species.



In the case of our experiment, the heating was both low temperature and short in duration; therefore the possibility further hydrogen releasing cross-linking reactions can be rejected. Indeed, previous NMR experiments have shown previously that PABs and BZ rapidly form in AB-PEO composites with low AB content at low temperatures with cross-linking occurring upon prolonged heating at higher temperatures.⁶

All together the thermolytic processes described account for the release of between 1-2 equivalents of H_2 . But, since **1** contains no B–H bonds, it is clear that further hydrogen releasing reactions must have taken place. Given the presence of B–O bonds in the final structure of the crystal it can be deduced that the polymeric residues from thermolysis must have undergone hydrolysis as a result of the action of adventitious water from the ambient atmosphere.

The hydrolysis of ammonia borane has been widely studied.⁷ It is well-known that solutions of ammonia borane are stable to hydrolysis under inert atmospheres, but become unstable due to the action of carbonic acid from the dissolution of CO_2 , or in the presence of acids.⁸ PABs and BZ are known to be much more sensitive to hydrolysis than AB and the hydrolysis of these species is

⁴ A. L. Spek, *Acta Crystallogr., Sect. C: Struct. Chem.*, 2014, **71**, 9–18; B. Rees, L. Jenner and M. Yusupov, *Acta Crystallogr. Sect. D: Biol. Crystallogr.*, 2005, **61**, 1299–1301.

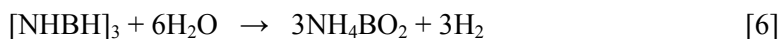
⁵ J. S. Wang and R. A. Geanangel, *Inorg. Chim. Acta*, 1988, **148**, 185–190; W. J. Shaw, J. C. Linehan, N. K. Szymczak, D. J. Heldebrant, C. Yonker, D. M. Camaioni, R. T. Baker and T. Autrey, *Angew. Chem., Int. Ed.*, 2008, **47**, 7493–7496; J. F. Kostka, R. Schellenberg, F. Baitalow, T. Smolinka and F. Mertens, *Eur. J. Inorg. Chem.*, 2012, **2012**, 49–54; Y. Kim, H. Baek, J. H. Lee, S. Yeo, K. Kim, S. J. Hwang, B. Eun, S. W. Nam, T. H. Lim and C. W. Yoon, *Phys. Chem. Chem. Phys.*, 2013, **15**, 19584–19594; S. Yeo, Y. Kim, J. H. Lee, K. Kim, J. H. Jang, S. A. Hong, S. W. Nam and C. W. Yoon, *Int. J. Hydrogen Energy*, 2014, **39**, 21786–21795; J. Li, C. Zhang, B. Li, F. Cao and S. Wang, *Inorg. Chim. Acta*, 2011, **366**, 173–176.

⁶ A. R. Ploszajski, M. Billing, A. S. Nathanson, M. Vickers and S. M. Bennington, *Int. J. Hydrogen Energy*, 2018, **43**, 5645–5656.

⁷ U. B. Demirci and P. Miele, *J. Power Sources*, 2010, **195**, 4030–4035; U. B. Demirci, *Int. J. Hydrogen Energy*, 2017, **42**, 9978–10013; G. Moussa, R. Moury, U. B. Demirci and P. Miele, *Int. J. Hydrogen Energy*, 2013, **38**, 7888–7895.

⁸ M. Chandra and Q. Xu, *J. Power Sources*, 2006, **159**, 855–860.

described in Eq. 5 and 6, indicating the formation of hydrogen and ammonium borate. It should be noted that the hydrolysis products are also known to accelerate the hydrolysis process.



These two equations do not capture the whole picture though, since aqueous borate solutions are known to contain a number of borate species in complex equilibria with each other depending on factors such as pH, boron concentration and temperature. Perhaps the most important hydrolysis products, from the viewpoint of this study, are formed by the addition of water to ammonium borate creating an equilibrium with the products boric acid and ammonia (Eq. 7).



A further equilibrium is established by the addition of a further water molecule to ammonia and boric acid, forming ammonium tetrahydroxyborate.



It is this tetrahedral tetrahydroxyborate species which is crucial to the formation of ammonium pentaborate. Condensation reactions between the tetrahydroxyborate anion and neutral boric acid moieties release water molecules to yield the pentaborate anion (Eq. 9) with its tetrahedral B₃ centre. The pentaborate anion is common in naturally occurring soroborate minerals and, unlike some other borates, is known to crystallise easily from solution.⁹



This sequence of reactions explains how the ammonium pentaborate species is produced. The formation of a supramolecular crystalline structure requires the polyethylene glycol (PEG) molecules. These PEG molecules extend through four channels in each unit cell, and each channel contains two ammonium ions which extend towards the centre of the channels. These ammonium ions form hydrogen bonds with ether oxygen atoms in the polymer to provide stability to the supramolecular structure. Guest molecules can be used as templates to create large voids in the synthesis of other framework structures such as zeolites¹⁰ and metal organic frameworks.¹¹

⁹ V. R. Hathwar, A. K. Paul, S. Natarajan and T. N. Guru Row, *J. Phys. Chem. A*, 2011, **115**, 12818–12825.

¹⁰ A. Sachse and J. Garcia-Martinez, *Chem. Mater.* 2017, **29**, 3827.

¹¹ C. Duan, F. Li, H. Zhang, J. Li, X. Wang and H. Xi, *RSC Adv.* 2017, **7**, 52245.

Table S1. Crystal data and structure refinement for $\text{NH}_4\text{B}_5\text{O}_6(\text{OH})_4 \cdot (\text{C}_2\text{H}_4\text{O})_x$ at 150 K.

Identification code	exp_1071
Empirical formula	$\text{NH}_4\text{B}_5\text{O}_6(\text{OH})_4 \cdot (\text{C}_2\text{H}_4\text{O})_x$
Formula weight	236.12 (*)
Temperature / K	150
Crystal system	monoclinic
Space group	$P2_1/c$
a / Å	9.2922(2)
b / Å	17.3394(5)
c / Å	16.3648(5)
α / °	90
β / °	91.234(2)
γ / °	90
Volume / Å ³	2636.12(13)
Z	8
ρ_{calc} / g cm ⁻³	1.190 (*)
μ / mm ⁻¹	1.040 (*)
$F(000)$	960 (*)
Crystal size / mm ³	0.091 × 0.081 × 0.02
Radiation	CuKα ($\lambda = 1.54184$ Å)
2θ range for data collection / °	7.428 to 147.128
Index ranges	$-11 \leq h \leq 7, -21 \leq k \leq 21, -17 \leq l \leq 19$
Reflections collected	10626
Independent reflections	5140 [$R_{\text{int}} = 0.0254, R_{\text{sigma}} = 0.0331$]
Data/restraints/parameters	5140/94/322
Goodness-of-fit on F^2	1.002
Final R indexes [$I \geq 2\sigma(I)$]	$R_1 = 0.0383, wR_2 = 0.1048$
Final R indexes [all data]	$R_1 = 0.0492, wR_2 = 0.1117$
Largest diff. peak/hole / e Å ⁻³	0.16/-0.20

*excluding contribution from unknown amount of polyethylene oxide. Assuming 3.5 monomer units of PEG per 2 units of $\text{NH}_4\text{B}_5\text{O}_6(\text{OH})_4$ given void volume and electron count from squeeze, the formula weight increases to 313.21.

Table S2. Fractional atomic coordinates ($\times 10^4$) and equivalent isotropic displacement parameters ($\text{\AA}^2 \times 10^3$) for $\text{NH}_4\text{B}_5\text{O}_6(\text{OH})_4 \cdot (\text{C}_2\text{H}_4\text{O})_x$ at 150 K. U_{eq} is defined as $\frac{1}{3}$ of the trace of the orthogonalised U_{ij} tensor.

Atom	x	y	z	U(eq)
O(1A)	7339.7(10)	3865.5(7)	4038.5(6)	28.9(2)
O(2A)	4889.4(10)	4093.7(8)	4360.3(7)	33.9(3)
O(3A)	6607.9(10)	3889.8(7)	5446.1(6)	28.1(2)
O(4A)	9037.2(10)	4162.2(6)	5092.7(7)	28.0(2)
O(5A)	10635.0(11)	3092.0(7)	5020.0(8)	38.1(3)
O(6A)	8093.5(10)	2867.8(6)	4979.6(7)	29.4(2)
O(7A)	9783.7(12)	1839.2(7)	5138.9(9)	41.0(3)
O(8A)	11562.9(11)	4342.8(7)	5079.9(9)	38.8(3)
O(9A)	5660.6(11)	4318.3(8)	3032.8(7)	35.4(3)
O(10A)	4192.3(11)	4060.5(8)	5749.1(7)	37.6(3)
B(1A)	5989.3(17)	4086.4(11)	3809.0(11)	29.5(3)
B(2A)	5223.7(17)	4006.4(11)	5183.9(11)	28.6(3)
B(3A)	7756.2(16)	3691.0(10)	4893.6(11)	26.2(3)
B(4A)	10395.8(17)	3874.7(11)	5055.7(12)	30.5(4)
B(5A)	9464.5(17)	2598.9(11)	5045.3(11)	30.7(4)
O(1B)	1875.1(10)	5645.6(7)	7889.3(6)	30.3(2)
O(2B)	-620.0(11)	5349.7(9)	8010.9(7)	40.0(3)
O(3B)	952.4(10)	5156.1(7)	9155.5(6)	28.1(2)
O(4B)	2639.4(10)	6178.2(7)	9184.6(7)	29.3(2)
O(5B)	5117.7(10)	5823.3(7)	9245.2(7)	31.4(2)
O(6B)	3371.4(10)	4899.0(6)	8788.8(6)	28.4(2)
O(7B)	5801.2(11)	4569.3(8)	8822.4(8)	38.4(3)
O(8B)	4412.2(11)	7008.1(7)	9776.3(8)	36.4(3)
O(9B)	248.4(12)	5689.3(10)	6746.6(7)	48.3(4)
O(10B)	-1551.9(11)	4999.1(9)	9268.9(7)	42.3(3)
B(1B)	541.2(18)	5572.8(13)	7547.1(11)	34.3(4)
B(2B)	-390.4(18)	5167.7(12)	8819.5(11)	32.3(4)
B(3B)	2221.5(16)	5470.5(11)	8750.1(10)	26.6(3)
B(4B)	4023.3(17)	6339.6(11)	9401.8(11)	28.4(3)
B(5B)	4767.5(17)	5095.5(11)	8949.3(10)	27.9(3)
N(1)	2784.2(16)	1642.9(10)	4380.4(10)	45.4(4)
N(2)	3008(2)	5201.8(13)	3126.4(13)	67.8(6)
H(1A)	2887(17)	1110(4)	4276(9)	96(4)
H(1B)	2764(16)	1916(8)	3881(5)	96(4)
H(1C)	3568(11)	1816(8)	4708(7)	96(4)
H(1D)	1917(9)	1730(9)	4657(8)	96(4)
H(2A)	3009(17)	5425(8)	3653(5)	96(4)
H(2B)	3862(10)	4915(7)	3062(10)	96(4)
H(2C)	2205(10)	4872(6)	3062(9)	96(4)

H(2D)	2958(16)	5595(6)	2728(7)	96(4)
H(7A)	9035	1596	5257	62
H(8A)	11293	4805	5082	58
H(9A)	6420	4357	2767	53
H(10A)	3386	4112	5514	56
H(7B)	6604	4752	8967	58
H(8B)	3682	7287	9834	55
H(9B)	1022	5726	6494	72
H(10B)	-1293	4935	9759	64

Table S3. Anisotropic displacement parameters ($\text{\AA}^2 \times 10^3$) for $\text{NH}_4\text{B}_5\text{O}_6(\text{OH})_4 \cdot (\text{C}_2\text{H}_4\text{O})_x$ at 150 K. Anisotropic displacement factor exponent has the form: $-2\pi^2[h^2a^{*2}U_{11}+2hka^{*}b^{*}U_{12}+\dots]$.

Atom	U_{11}	U_{22}	U_{33}	U_{23}	U_{13}	U_{12}
O(1A)	17.8(4)	42.3(6)	26.6(5)	5.6(4)	1.3(4)	4.0(4)
O(2A)	17.3(5)	55.7(7)	28.5(6)	6.5(5)	-0.6(4)	3.7(5)
O(3A)	16.7(4)	40.7(6)	26.7(5)	2.4(4)	-0.3(4)	2.3(4)
O(4A)	16.0(4)	32.3(5)	35.5(6)	3.3(4)	-1.1(4)	1.4(4)
O(5A)	17.5(5)	34.4(6)	62.5(8)	4.8(5)	1.9(5)	2.8(4)
O(6A)	18.6(5)	32.4(6)	37.1(6)	4.9(4)	-1.3(4)	1.0(4)
O(7A)	22.9(5)	33.8(6)	66.4(8)	6.9(6)	1.2(5)	2.5(4)
O(8A)	16.4(5)	34.6(6)	65.1(8)	5.7(6)	-3.8(5)	2.3(4)
O(9A)	22.9(5)	57.1(8)	26.0(6)	5.8(5)	-1.7(4)	4.6(5)
O(10A)	18.8(5)	62.5(8)	31.4(6)	3.5(5)	1.4(4)	5.2(5)
B(1A)	19.6(7)	39.4(9)	29.4(8)	3.2(7)	-1.6(6)	2.3(7)
B(2A)	17.7(7)	37.3(9)	30.8(9)	3.4(7)	-1.0(6)	1.0(6)
B(3A)	16.6(6)	34.7(9)	27.2(8)	2.8(6)	-0.5(6)	1.4(6)
B(4A)	18.1(7)	35.5(9)	37.6(9)	4.7(7)	-2.0(6)	2.9(7)
B(5A)	20.7(7)	34.7(9)	36.6(9)	3.0(7)	0.1(6)	1.8(7)
O(1B)	18.7(5)	47.6(6)	24.6(5)	3.3(4)	-0.8(4)	-3.4(4)
O(2B)	17.9(5)	75.4(9)	26.5(6)	8.3(6)	-3.0(4)	-7.2(5)
O(3B)	16.7(4)	43.8(6)	23.7(5)	2.2(4)	-0.7(4)	-2.8(4)
O(4B)	17.5(4)	38.4(6)	32.0(6)	-4.1(4)	-2.5(4)	0.0(4)
O(5B)	15.9(4)	41.2(6)	37.0(6)	-5.7(5)	-2.5(4)	-2.3(4)
O(6B)	17.6(5)	36.8(6)	30.6(5)	-3.5(4)	-1.8(4)	-1.2(4)
O(7B)	19.1(5)	43.4(7)	52.5(7)	-10.6(6)	-5.1(5)	2.1(5)
O(8B)	23.9(5)	38.0(6)	47.0(7)	-7.4(5)	-5.9(5)	0.5(4)
O(9B)	23.1(5)	96.3(12)	25.5(6)	9.9(6)	-3.2(4)	-6.1(6)
O(10B)	16.9(5)	82.8(10)	27.2(6)	9.3(6)	-2.3(4)	-6.8(5)
B(1B)	20.3(7)	55.9(12)	26.6(9)	2.6(8)	-1.6(6)	-3.5(8)
B(2B)	20.0(7)	49.4(11)	27.3(9)	1.9(7)	-0.7(6)	-3.7(7)
B(3B)	17.3(7)	39.9(9)	22.5(8)	-1.0(7)	-0.4(6)	-2.6(6)
B(4B)	20.1(7)	38.1(9)	27.0(8)	-0.2(7)	0.1(6)	-1.2(7)
B(5B)	19.2(7)	37.5(9)	27.0(8)	-1.2(7)	0.6(6)	-1.9(6)
N(1)	41.3(8)	47.1(9)	47.1(9)	-3.4(7)	-10.8(7)	11.9(7)
N(2)	61.2(11)	73.4(13)	67.0(12)	-28.4(10)	-37.7(10)	33.0(10)

Table S4. Selected bond lengths for $\text{NH}_4\text{B}_5\text{O}_6(\text{OH})_4 \cdot (\text{C}_2\text{H}_4\text{O})_x$ at 150 K.

Atom — Atom	Length / Å	Atom — Atom	Length / Å
O(1A) — B(1A)	1.357(2)	O(1B) — B(1B)	1.355(2)
O(1A) — B(3A)	1.475(2)	O(1B) — B(3B)	1.470(2)
O(2A) — B(1A)	1.378(2)	O(2B) — B(1B)	1.388(2)
O(2A) — B(2A)	1.385(2)	O(2B) — B(2B)	1.373(2)
O(3A) — B(2A)	1.362(2)	O(3B) — B(2B)	1.353(2)
O(3A) — B(3A)	1.455(2)	O(3B) — B(3B)	1.470(2)
O(4A) — B(3A)	1.474(2)	O(4B) — B(3B)	1.466(2)
O(4A) — B(4A)	1.360(2)	O(4B) — B(4B)	1.360(2)
O(5A) — B(4A)	1.377(2)	O(5B) — B(4B)	1.383(2)
O(5A) — B(5A)	1.385(2)	O(5B) — B(5B)	1.388(2)
O(6A) — B(3A)	1.467(2)	O(6B) — B(3B)	1.458(2)
O(6A) — B(5A)	1.359(2)	O(6B) — B(5B)	1.361(2)
O(7A) — B(5A)	1.358(2)	O(7B) — B(5B)	1.344(2)
O(8A) — B(4A)	1.354(2)	O(8B) — B(4B)	1.357(2)
O(9A) — B(1A)	1.361(2)	O(9B) — B(1B)	1.347(2)
O(10A) — B(2A)	1.349(2)	O(10B) — B(2B)	1.351(2)

Table S5. Selected bond angles for $\text{NH}_4\text{B}_5\text{O}_6(\text{OH})_4 \cdot (\text{C}_2\text{H}_4\text{O})_x$ at 150 K.

Atom — Atom — Atom	Angle / °	Atom — Atom — Atom	Angle / °
B(1A) — O(1A) — B(3A)	122.85(12)	B(1B) — O(1B) — B(3B)	123.80(12)
B(1A) — O(2A) — B(2A)	118.83(12)	B(2B) — O(2B) — B(1B)	119.01(13)
B(2A) — O(3A) — B(3A)	122.66(12)	B(2B) — O(3B) — B(3B)	123.56(13)
B(4A) — O(4A) — B(3A)	122.20(13)	B(4B) — O(4B) — B(3B)	122.65(12)
B(4A) — O(5A) — B(5A)	118.67(12)	B(4B) — O(5B) — B(5B)	119.04(12)
B(5A) — O(6A) — B(3A)	122.64(12)	B(5B) — O(6B) — B(3B)	122.20(13)
O(1A) — B(1A) — O(2A)	121.06(14)	O(1B) — B(1B) — O(2B)	121.00(15)
O(1A) — B(1A) — O(9A)	121.95(14)	O(9B) — B(1B) — O(1B)	123.48(15)
O(9A) — B(1A) — O(2A)	116.99(13)	O(9B) — B(1B) — O(2B)	115.50(14)
O(3A) — B(2A) — O(2A)	120.88(13)	O(3B) — B(2B) — O(2B)	121.21(14)
O(10A) — B(2A) — O(2A)	120.78(13)	O(10B) — B(2B) — O(2B)	117.71(14)
O(10A) — B(2A) — O(3A)	118.31(14)	O(10B) — B(2B) — O(3B)	121.08(15)
O(3A) — B(3A) — O(1A)	111.10(12)	O(1B) — B(3B) — O(3B)	110.36(11)
O(3A) — B(3A) — O(4A)	109.32(13)	O(4B) — B(3B) — O(1B)	110.00(14)
O(3A) — B(3A) — O(6A)	109.20(13)	O(4B) — B(3B) — O(3B)	107.34(12)
O(4A) — B(3A) — O(1A)	106.86(12)	O(6B) — B(3B) — O(1B)	109.10(12)
O(6A) — B(3A) — O(1A)	109.97(13)	O(6B) — B(3B) — O(3B)	108.83(13)
O(6A) — B(3A) — O(4A)	110.37(11)	O(6B) — B(3B) — O(4B)	111.20(12)
O(4A) — B(4A) — O(5A)	120.94(14)	O(4B) — B(4B) — O(5B)	120.99(15)
O(8A) — B(4A) — O(4A)	121.50(15)	O(4B) — B(4B) — O(8B)	122.46(15)
O(8A) — B(4A) — O(5A)	117.52(13)	O(8B) — B(4B) — O(5B)	116.55(13)
O(6A) — B(5A) — O(5A)	121.43(15)	O(6B) — B(5B) — O(5B)	120.67(14)
O(7A) — B(5A) — O(5A)	115.62(13)	O(7B) — B(5B) — O(5B)	120.54(13)
O(7A) — B(5A) — O(6A)	122.95(15)	O(7B) — B(5B) — O(6B)	118.78(15)

Table S6. Solvent mask information for $\text{NH}_4\text{B}_5\text{O}_6(\text{OH})_4 \cdot (\text{C}_2\text{H}_4\text{O})_x$. From a combination of void volume and electron count, it is estimated that there are approximately 3.5 monomer units of $-\text{CH}_2\text{CH}_2\text{O}-$ per 2 units of $\text{NH}_4\text{B}_5\text{O}_6(\text{OH})_4$.

No.	x	y	z	$V / \text{\AA}^3$	electrons	content
1	-0.740	0.225	0.246	215.7	75.4	3.5($\text{C}_2\text{H}_4\text{O}$)
2	-0.838	0.275	0.746	215.7	75.4	3.5($\text{C}_2\text{H}_4\text{O}$)
3	-0.110	0.725	0.254	215.7	75.4	3.5($\text{C}_2\text{H}_4\text{O}$)
4	-0.495	0.775	0.754	215.7	75.4	3.5($\text{C}_2\text{H}_4\text{O}$)

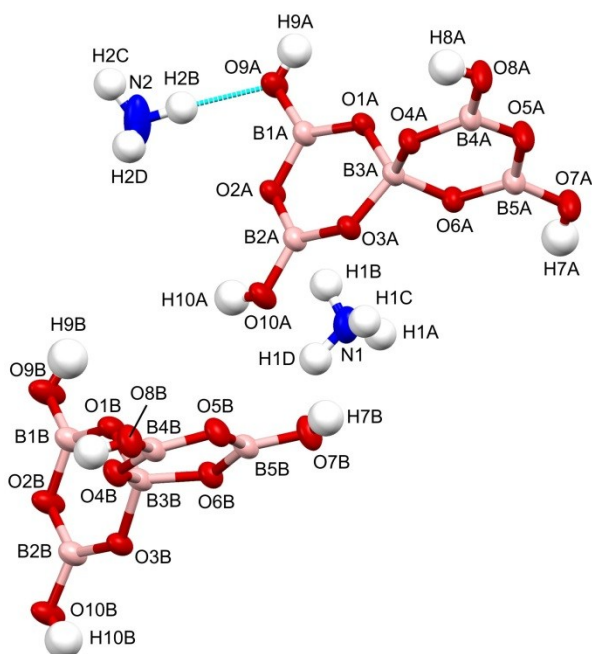


Fig. S1. Motif of the crystal showing the labelling scheme of the atoms. Thermal ellipsoids are shown at 50% probability at 150 K.

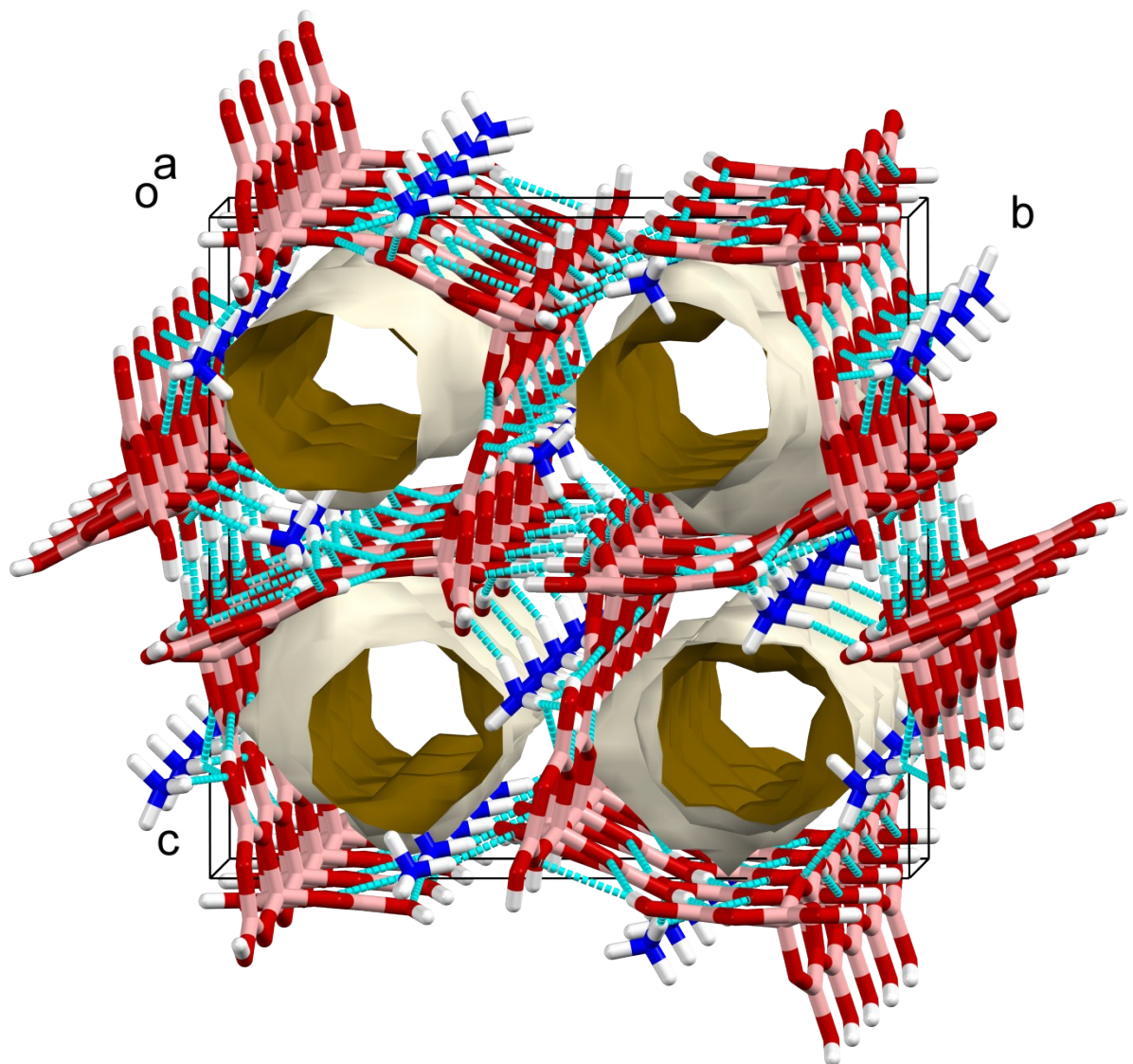


Fig. S2. View along **a** in the crystal showing the PEO containing channels. The extensive hydrogen bonded network of pentaborate anion (pink and red) is shown in cyan. The ammonium cations link both pentaborate anions and the PEO within the channels.

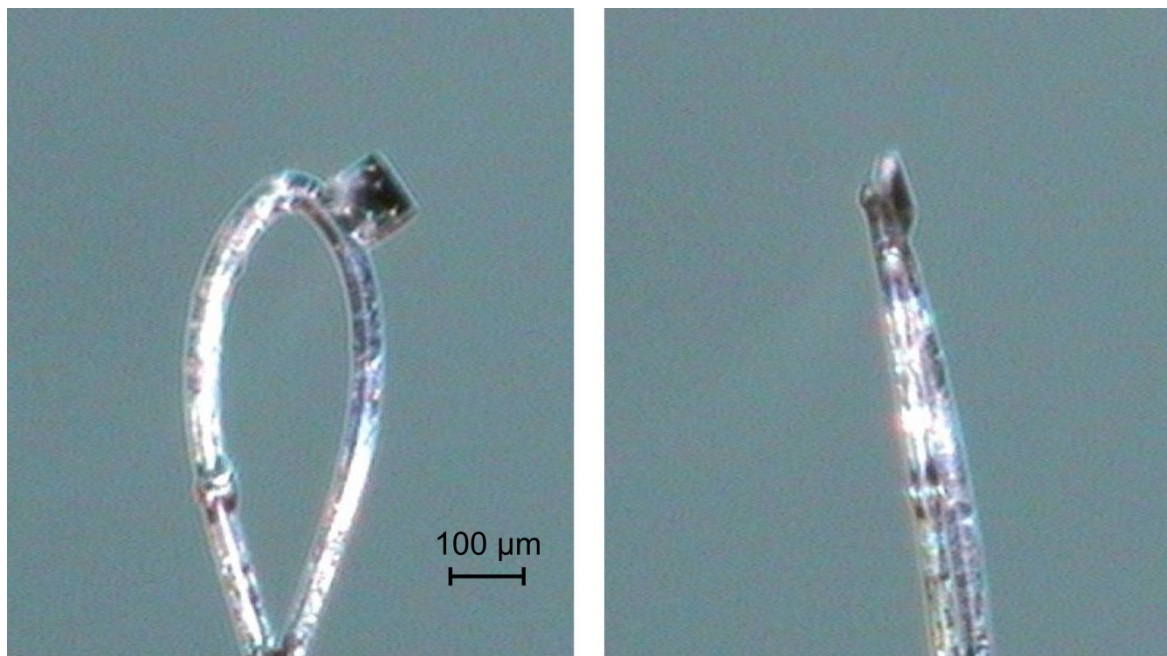


Fig. S3. Two views of the crystal used for the single-crystal study held in a Hampton Research nylon loop. The crystal habit is a square flat plate with dimensions $91 \times 81 \times 20 \mu\text{m}^3$.